Tracing the Reactive Melting of Glass-Forming Silicate Batches by In Situ ^{23}Na NMR

Aled R. Jones,[†,‡] Rudolf Winter,*[,†] Pierre Florian,[§] and Dominique Massiot[§]

Materials Physics, University of Wales Aberystwyth, Penglais, Aberystwyth SY23 3BZ, Wales, U.K., and CNRS Centre de Recherche sur les Matériaux à Haute Température, 1D avenue de la Recherche Scientifique, 45071 Orléans Cedex 2, France

Received: September 21, 2004; In Final Form: December 20, 2004

The kinetics of the reaction of batches of powdered quartz and sodium carbonate was studied by in situ ^{23}Na nuclear magnetic resonance (NMR) spectroscopy using a laser-heated probe. We show for the first time that the technique allows one to study solid-state reactions at high temperatures with good time resolution and without the risk of quenching artifacts. The reaction is controlled by solid-state Na^+ diffusion across the grain interface. Independent of the batch composition, the first reaction product is crystalline sodium metasilicate, Na_2SiO_3, even if the temperature is high enough for much of the composition space between silica and metasilicate to be above the equilibrium liquidus. Fast Na^+ diffusion allows the reaction front to cross the grain interface and form the solid product before liquid intermediate equilibrium products can be formed. This purely solid-state reaction slows down as the thickness of the interface increases; the reaction is more deceleratory than published models suggest. If excess quartz is present, it reacts in a second step involving a liquid film wetting the excess grains. Once this reaction has started, it pulls the reaction into the thermodynamic regime, which leads to an increase even in the rate of the first step leading to intermediate solid metasilicate.

1. Introduction

Nuclear magnetic resonance (NMR) spectroscopy is a technique that allows one to study atomic structures and processes in bulk samples by exploiting its sensitivity to the local environment of a particular nuclide. Its usefulness as a technique for in situ measurements of processes such as phase transitions and chemical reactions with good time resolution is widely applied in problems involving liquid samples near room temperature. Solid-state NMR usually relies on magic angle spinning (MAS) to achieve sufficient spectral resolution to characterize different sites and phases. When dealing with hard condensed matter, phase transitions and reactions generally involve high temperatures. Unfortunately, even with specialist probes,[1] MAS is currently only possible up to ~700 °C and only at spinning speeds that would not be sufficient to deal with the line widths of many quadrupolar nuclei because there are no container materials whose mechanical strength is sufficient at high temperatures to allow fast spinning. As a consequence, NMR studies of glasses[2−8] and refractories[9−11] are generally limited to ex situ measurements of samples subjected to thermal treatment which are subsequently quenched. This limits the time resolution and introduces some degree of uncertainty as to whether any phases detected are genuine reaction products or merely quenching artifacts, for example, due to recrystallization. In situ NMR experiments at high temperatures avoid these problems but at the price of lower spectral resolution in any given time slice. This is not a problem if sharp phase transitions with a very distinct change in line shape are observed. In this paper, we show that it is not necessarily a problem either when dealing with gradual spectral changes induced by chemical reactions as long as the individual phases are characterized independently. While previous high-temperature NMR experiments were focused on recrystallization from the melt,[12] speciation equilibria in the melt,[13] chemical reaction in the melt phase,[14] or structural premelting effects of stoichiometric crystals,[15] we report here for the first time an application of the technique to solid-state diffusion-driven reaction kinetics.

The laser-heating technique employed here has the advantage that it avoids electrical interference from circuitry necessary for resistance heating. It also provides the opportunity to reach extreme temperatures necessary for research into refractories. The setup can be modified to produce either very homogeneous heating by aerodynamically levitating a drop or spherical solid sample or, in the opposite extreme, very steep temperature gradients. The latter is useful if the structural response of thermal barrier materials is to be investigated.

In this study, we are dealing with the reactions between grains of quartz and sodium carbonate. The system is used as a physical model for batches typical of those used in the glass-making industry. It is important to know to what extent batch reactions are controlled by kinetics and thermodynamics, respectively, as this allows one to optimize the heat profile of a float line and reduce both energy consumption and emissions. Where, as in this case, ionic diffusion in the solid state plays an important role, the grain size and the structural detail of grain interfaces are factors that can tip the balance in favor of one particular mechanism or another. This, again, is technologically relevant, and the reduction in grain size of raw material and a careful balancing of particle sizes of the various raw materials may be both ecologically beneficial and economically viable.

It is useful to recall some details of the phase diagram of the system Na_2O-SiO_2.[16] In this study, Na_2CO_3 is actually used

* To whom correspondence should be addressed. Phone: +44-1970-621797. Fax: +44-1970-622826. E-mail: ruw@aber.ac.uk.
† University of Wales Aberystwyth.
‡ Present address: Pilkington plc, European Technical Centre, Lathom, Ormskirk L40 5UF, England, U.K.
§ CNRS-CRMHT Orléans.

10.1021/jp045705s CCC: $30.25
Published on Web 02/15/2005

TABLE 1: Melting Points of Eutectics and Stoichiometric Compounds in the System xNa$_2$O−(1 − x)SiO$_2$ (after ref 16)

x_{Na_2O}	T_m/°C	
0.000	870	quartz−tridymite transition
0.255	793	eutectic between disilicate and silica
0.333	874	disilicate
0.372	846	eutectic between metasilicate and disilicate
0.500	1089	metasilicate

instead of Na_2O, but as it is confined to the silica-rich side of the composition space, the melting points listed in Table 1 remain valid.

Of the four NMR-active nuclei in the system, ^{29}Si combines a relatively long relaxation time with a rather low abundance. The time resolution of ^{29}Si high-temperature NMR can be as good as about 1 min[18] but only at a signal-to-noise level that would not be sufficient to distinguish phases in a system as complex as a partially reacted batch. Both ^{13}C and ^{17}O would need to be enriched, which is prohibitively expensive in the case of oxygen for a destructive experiment such as this. ^{13}C has been used previously,[17] and it was shown that it leaves the batch at too early a stage to be useful to trace the entire reaction. Fortunately, ^{23}Na is an ideal nucleus for an in situ study, as it is abundant and has a reasonably large gyromagnetic ratio and short relaxation time. The only drawback is that, being a quadrupolar nucleus, it has a rather complicated intrinsic line shape. This problem can be overcome, though, by an adaptive fitting procedure using constraints obtained from a few ex situ experiments.

2. Experimental Section

The two main samples studied in this investigation were batches (powder mixtures) of quartz and sodium carbonate with a molar ratio of 1:1 ("metasilicate batch", $Na_2O{\cdot}SiO_2$) and 2:1 ("disilicate batch", $Na_2O{\cdot}2SiO_2$). In addition, the raw material, sodium carbonate (Na_2CO_3), and completely reacted, recrystallized metasilicate (Na_2SiO_3) and disilicate ($Na_2Si_2O_5$) were also used for reference. In this paper, the sum formulas are only used to refer to the fully reacted products, not the batches. Batches and reference samples were prepared from sieved high-purity natural quartz with a grain size between 63 and 90 μm and reagent grade Na_2CO_3 with a grain size of up to 300 μm. Crystalline reference samples were prepared by heating the stoichiometric batch in a vertical tube furnace to 1350 °C for 4 h, after which the temperature was gradually ramped down to 800 °C over a period of 16 h.

The in situ experiments were carried out at the CRMHT on a Bruker Avance400 spectrometer and a 9.4 T cryomagnet. A Bruker-CRMHT probe[19−22] with a vertical saddle coil was used. The samples were placed in boron nitride screw cap containers with an inner diameter of 5 mm and a wall thickness of 1 mm which are rested on a cylindrical yttria tube inside the probe. The sample container is heated by a 120 W CO_2 laser from underneath. The output of the laser can be controlled in steps of 1%. The relationship between output power and temperature is known by calibration using a sample container loaded with the tip of a thermocouple. However, because of the different thermal properties of the thermocouple and real samples, the calibration curve needs to be pegged to known fixed points. In this case, the melting points of pure Na_2CO_3 and Na_2SiO_3 (854 and 1089 °C) were used for this purpose.

The in situ spectra are calibrated against 1mol/L NaCl solution in water at room temperature. A $\pi/12$ pulse of 8 μs and a recycle delay of 460 ms were used, allowing a 1 min time resolution averaging over 128 scans per time slice. The small tip angle ensures that the excitation of the solid components is not affected by the quadrupolar coupling. The spectral width was 50 kHz. All heating experiments were conducted as isothermally as possible; that is, the laser power was set at the beginning of data acquisition and then left for the entire run. However, it was necessary at the beginning of each experiment to allow the sample to heat up for ∼3 min. High-temperature experiments were carried out at 815, 835, 855, and 880 °C with metasilicate batches and at 880 °C with a disilicate batch. The disilicate experiment was carried out twice for different periods in order to obtain samples quenched near the end of the reaction (after 120 min) and halfway through (after 39 min).

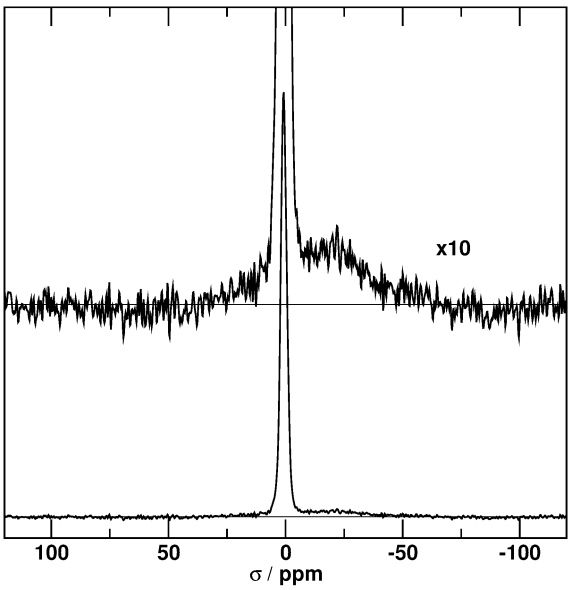

Figure 1. Spectrum of liquid Na_2CO_3. The top trace is a 10-fold magnification of the baseline, showing the ^{23}Na background signal from the probe. This is taken into account when modeling the batch spectra.

The high-temperature probe has a small ^{23}Na background signal. This is measured by taking a high-temperature spectrum of liquid Na_2CO_3 (cf. Figure 1). The spectrum of the reference sample is sufficiently narrow to differentiate the background from it. A direct measurement of the background in an empty probe would give rise to a larger error because of the different characteristics of the oscillating circuit of the probe due to the reduced filling factor of the coil. The background peak observed in Figure 1 is included in all fits to high-temperature spectra obtained in this study.

The ex situ MAS spectra of the in situ reacted samples were taken on another Bruker Avance400 spectrometer with 9.4 T cryomagnet at UWA. The pulse length was 0.5 μs, the recycle delay 1 s, and the spectral width 300 kHz.

MAS spectra confirm that laser-melted and subsequently recrystallized Na_2SiO_3 is structurally identical to material prepared conventionally.

3. Results

3.1. Reference Measurements: Raw Materials and Pure Products. Temperature-dependent reference spectra were taken of Na_2CO_3, Na_2SiO_3, and $Na_2Si_2O_5$. The objective of these is to generate constraints for the fitting procedure of the in situ spectra of the batches.

Spectra of pure Na_2CO_3 at high temperatures are shown in Figure 2a. At 740 °C, a broad static solid-state line shape is obtained. With increasing temperature, the line narrows progressively due to motional averaging. The line shape at 880 °C

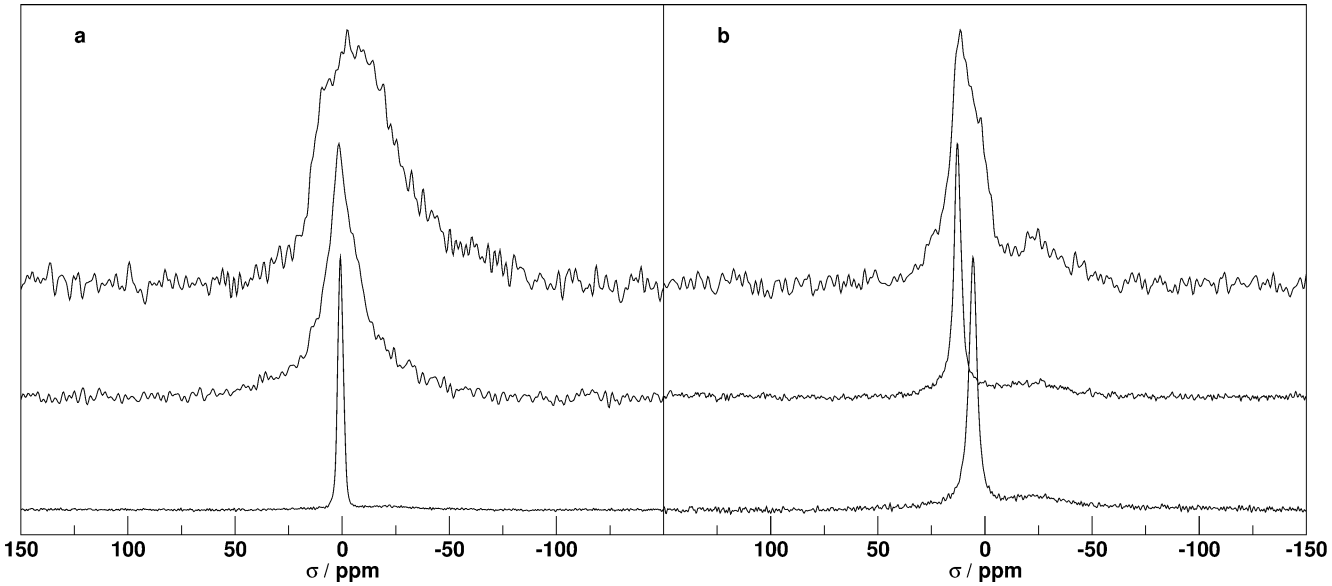

Figure 2. Reference spectra of (a) the raw material Na_2CO_3 at (top to bottom) 740, 830, and 880 °C and (b) the homogeneous products (top to bottom) metasilicate at 840 and 1090 °C and disilicate at 760 °C. The peak positions of the lines of the liquids are 0.8, 12, and 6 ppm, respectively. All spectra are scaled to have the same amplitude, hence the different signal-to-noise ratio.

corresponds to liquid Na_2CO_3. At lower temperatures than these (not shown), the spectra pass through a stage (near 400 °C) where a well-resolved doublet is observed. This doublet spectrum is representative of the room-temperature phase of Na_2CO_3 with motional narrowing averaging the exchange between sites but not the local electric field gradient. Na_2CO_3 undergoes a phase transition at 480 °C,[23] resulting in the 740 °C spectrum shown. The position of the pure liquid sodium carbonate line is 0.8 ppm.

High-temperature spectra of the two fully reacted products are shown in Figure 2b. The narrow lines of metasilicate at 1090 °C and disilicate at 760 °C prove that these products are entirely molten. The peak positions are 12 ppm for metasilicate and 6 ppm for disilicate. Due to the narrower lines, peak positions can be extracted with a higher accuracy from the spectra of the liquids. The solid-state metasilicate spectrum (at 840 °C) indicates that the peak positions observed with the liquids apply equally to the high-temperature solids. The high-temperature spectra of the reference compounds remain stable over time at constant laser power after the initial heating-up period of ∼3 min.

3.2. Metasilicate Batches: Na_2CO_3·SiO_2. The batch spectra evolve from the Na_2CO_3 line shape (as this is the only sodium containing component of the batch at the beginning) toward a product spectrum. Complete reaction was observed in no case (unless the whole sample was melted). Figure 3 shows a contour plot of all data obtained at 855 °C. The center of gravity of the peak shifts to the left, while a distinct narrow component begins to grow at the metasilicate position after ∼10 min. After ∼60 min, the spectra cease to change noticeably with time. The asymmetry of the line and the remaining broad component indicate however that some of the raw material remains unreacted. The same general behavior is observed at all four temperatures; only the time scale and the extent to which the broad line is diminished vary.

For each in situ experiment, a two-step fitting procedure was adopted. In the first step, several slices after different heating times were fitted with a set of Lorentzian lines as described below. After elimination of those parameters that showed little variance between these individual slices, the whole time-dependent data set was subjected to a collective fit to reveal

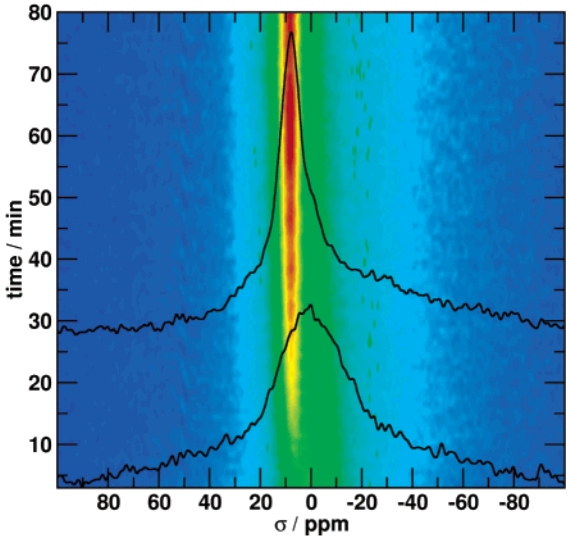

Figure 3. Evolution of metasilicate batch spectra at 855 °C with time (evolving from bottom to top). Each horizontal slice is averaged over a 1 min period. Amplitudes are color-coded. The two spectra shown in the foreground are the slices taken after 3 min and after 80 min, corresponding to the bottom and top slices in the two-dimensional plot in the background.

the exact time dependence of those parameters that do vary significantly with heating time. The whole fitting procedure was carried out using the NMR fitting program dmfit.[24] Figure 4 shows slice 20, that is, the spectrum measured 20 min into heating, of the metasilicate batch experiment at 815 °C as a typical example. The complex line shape resulting from the multicomponent nature of a partially reacted batch means that it is not possible to extract quadrupolar parameters for any site from the spectrum. However, the line shape is approximated by a superposition of four Lorentzian lines. Two of these represent reactant and product (without qualification at this stage as to which particular silicate phase it may be), respectively, and one is due to the probe background discussed earlier. The fourth component is designed to make up for the quadrupolar distortion of the carbonate and silicate lines, which cannot be adequately described by symmetric Lorentzian functions. The

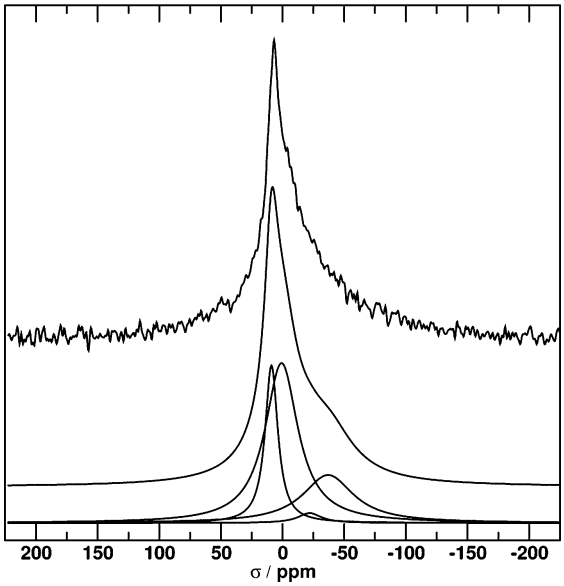

Figure 4. Typical metasilicate 1 min in situ spectrum. The line shape is modeled using four Lorentzian components for the reactant, the product, a quadrupolar tail component (see text for details), and the probe background.

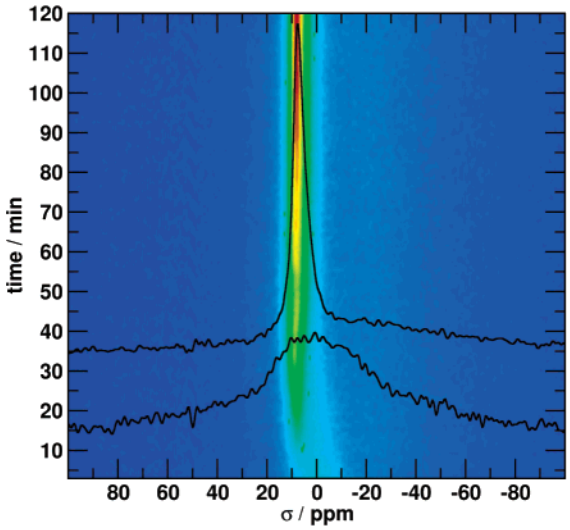

Figure 5. Evolution of disilicate batch spectra at 880 °C with time (evolving from bottom to top). Each horizontal slice is averaged over a 1 min period. Amplitudes are color-coded. The two spectra shown in the foreground are the slices taken after 3 min and after 120 min, corresponding to the bottom and top slices in the two-dimensional plot in the background.

curve fit therefore is intended not to justify directly a particular structural model on the atomic scale but to quantify the individual components present in the batch as a function of time. When interpreting the data, it will be necessary to take account of the "quadrupolar tail" component, as it contains intensity from spins located in both raw material and product. On the basis of the fits to individual slices and the independent probe background measurement, the positions of the four components were fixed at 0.8 ppm (carbonate), 9.0 ppm (silicate), −37.0 ppm (quadrupolar tail component), and −22.0 ppm (background). The widths of the components were fixed to 12.5 ppm (silicate), 50.0 ppm (tail), and 23.0 ppm (background). This leaves the collective fit to the entire in situ data set with five variable parameters: the width of the reactant line and the four amplitudes. The use of a fixed-width line shape for the final product and a variable-width line shape for the reactant component means that only ^{23}Na nuclei located in the pure final product contribute to the product line, while any intermediate environments resulting from a diffusion-limited solid-state reaction will be treated as part of the reactant fit component. This way, all Na^+ ions in environments that have not fully reacted are treated as reactant, and the width of the reactant line indicates the spread of Na^+ enviroments. However, such intermediate environments could alternatively be treated as part of the product fraction by allowing the product line width to vary while keeping the carbonate line width fixed.

3.3. Disilicate Batches: $Na_2CO_3 \cdot 2SiO_2$. The progressive changes in line shape of a disilicate batch over a 2 h period at 880 °C are illustrated in Figure 5. During the first 20 min, the spectra can be modeled in exactly the same way as the metasilicate ones. After this initial period, the disilicate batch develops a much narrower component near 11 ppm. The product line known from the metasilicate batches and this new one are too close to each other to be analyzed quantitatively as two separate components.

4. Discussion

With the reactant and product contributions separated, the kinetics of the reaction emerges. Figure 6a shows how the fractions of reactant, product, and quadrupolar tail components of the metasilicate batch spectra evolve with heating time at 855 °C. The fraction of spins in a particular environment is proportional to the integral of the corresponding spectral line. The quadrupolar tail component is not due to a separate site but contains spins in both carbonate and product environments. However, it is worth noting that the tail component remains fairly constant over time. Therefore, the use of Lorentzian lines representing the carbonate and product components does not cause a large error in terms of the kinetics of the reaction. This observation was made at all temperatures. The decrease of the carbonate component and increase of the product component are roughly exponential. This means that the reaction is more deceleratory than any of the mechanisms suggested in the literature.[25] Most popular mechanisms are based on the Ginstling−Brounshtein model,[26] which is built around a diffusion-controlled solid−liquid interface reaction. Even the most deceleratory mechanism,[27] which involves slow solid-state diffusion supplied from a solid−liquid interface of limited and shrinking cross-sectional area, does not level out to the same extent as the rate profiles measured here. Recently, a parametrized Ginstling−Brounshtein model was proposed[28] which allows predictive modeling of deceleratory glass batch reactions to some extent. Unfortunately, the parametrization means that it cannot be based on any particular atomistic notion. However, it is also possible to modify the Ginstling−Brounshtein model by introducing an explicit concentration dependence of the diffusion coefficient,[29] which can, depending on the conditions, make the kinetics more deceleratory.

With respect to the experiments reported here, however, it has to be noted that, as the samples are thermally rather insulating, a thermal gradient will exist within each of the samples such that the top layer of the sample is at a lower temperature than the main body, resulting in layers of material which have reacted to a different extent. Visual inspection of the samples at the end of the in situ experiment indicates that no completely unreacted material (loose grains) is left over. The absence of unreacted grains suggests that the deceleratory regime is not asymptotic toward a certain fixed fraction (as would be the case if there was a top layer which is so well insulated as never to become reactive) but simply that some part of the

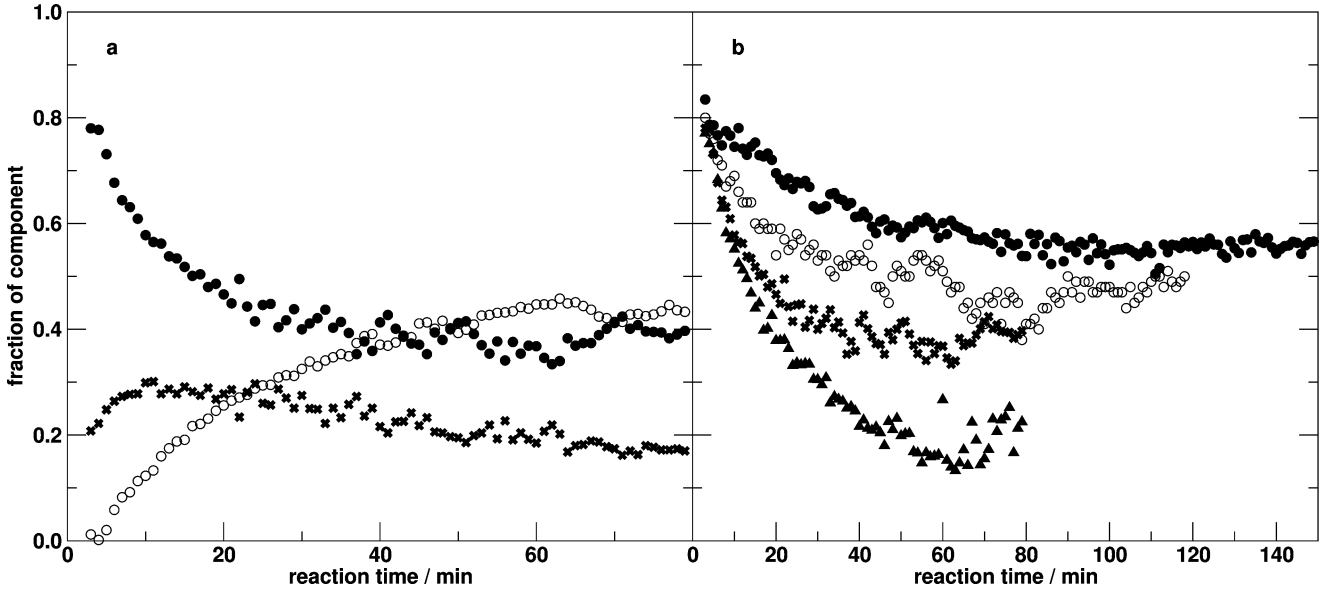

Figure 6. Development of the intensities of the spectral components (taking into account both amplitude and width) of metasilicate batches over time: (a) data for the reactant (●), metasilicate (○), and the quadrupolar tail component (×) from the experiment at 855 °C; (b) comparison of the reactant decay at 835 °C (●), 815 °C (○), 855 °C (×), and 880 °C (▲).

sample reacts slower because its temperature is lower than that indicated by the external calibration.

The decays of the carbonate component in each of the four in situ metasilicate batch experiments are compared in Figure 6b. The general observation is, as may be expected, that the raw material is consumed faster as the temperature increases. However, the measurement taken at 835 °C appears to be out of sequence, displaying a lower reaction rate than the one at 815 °C. This is probably caused by a difference in packing density, causing different thermal conductivity across the sample and therefore a different thermal gradient. This observation makes it clear that in situ thermometry would indeed be desirable in this kind of experiment.

The total amount of sample reacted (or carbonate unreacted) is determined independently by analyzing the last slices of each in situ experiment and by ex situ MAS spectroscopy of the final product. In the case of the data taken in situ, the actual reactant and product fractions are obtained by adding to the intensity of the corresponding fit component a fraction of the quadrupolar tail component given by the ratio of the reactant and product line intensities. This is necessary because the relative contribution of reactant to the quadrupolar tail component, which remains nearly constant over time, decreases as carbonate is consumed. The ex situ MAS spectra (cf. Figure 7) can be modeled with a three-site quadrupolar model. The line at $\sigma_{iso} = 21.6$ ppm is due to crystalline metasilicate in accordance with literature data.[30,31] Its quadrupole parameters are $C_q = 1.4 \pm 0.1$ MHz and $\eta_q = 0.7 \pm 0.1$. The room-temperature modification of sodium carbonate has two distinct sites, a symmetric and an asymmetric one,[32] giving rise to the two components at $\sigma_{iso} = 6.4$ ppm and $\sigma_{iso} = -1.5$ ppm, respectively. Their quadrupole parameters are $C_q = 1.2 \pm 0.1$ MHz at $\eta_q = 0$ (symmetric line) and $C_q = 2.5 \pm 0.1$ MHz at $\eta_q = 0.4 \pm 0.1$ (asymmetric line). The MAS spectra therefore allow one to identify the product phase without a doubt as pure sodium metasilicate. Since a line resembling the disilicate reference does not occur, it is obvious that metasilicate is formed directly, without an intermediate disilicate phase occurring. The fractions of remaining carbonate and formed metasilicate at the end of each experiment as obtained from analyzing the last slices of the in situ data and from the ex situ MAS spectra are listed in Table 2. Excellent agreement between both results is found at the higher temperatures. The discrepancies are somewhat larger, though, where the quadrupolar tail component is dominated by sodium carbonate with its more distorted Na^+ environment, as evidenced by the asymmetry parameter measured in the MAS experiments. The MAS spectrum obtained after the 835 °C experiment confirms that this batch has reacted to a lesser extent than expected according to its nominal temperature.

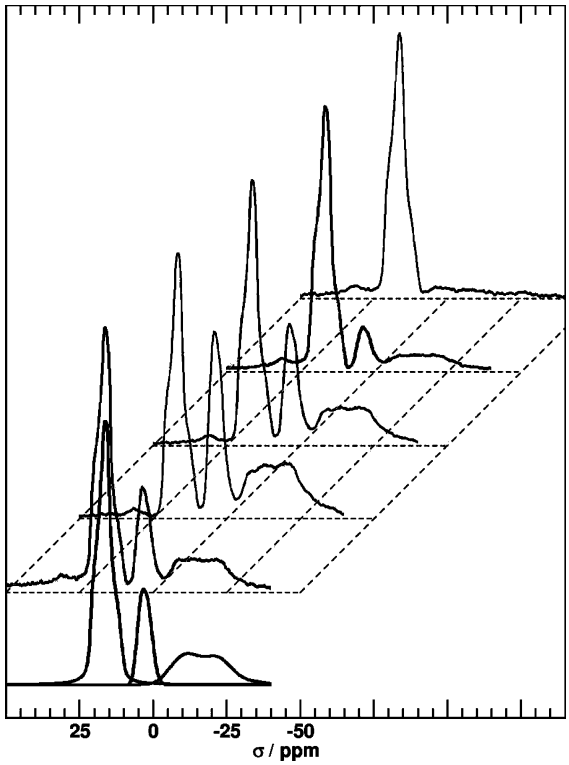

Figure 7. Ex situ ^{23}Na MAS NMR spectra of the batches after the end of the in situ experiments are shown in the top five traces, each shifted successively to the right by 25 ppm for clarity. The spectra were taken at room temperature after the in situ experiments at 815, 835, 855, and 880 °C (front to back). The top spectrum originates from a sample entirely melted during the in situ experiment. The unshifted bottom trace shows a three-site quadrupolar fit to the 815 °C spectrum.

TABLE 2: Fractions of Unreacted Na_2CO_3 and Reacted Metasilicate as Obtained from the Last Slice of the In Situ Experiments and from Later Ex Situ MAS Experiments (cf. Figure 7) of the Product[a]

	in situ		ex situ MAS	
sample	Na_2SiO_3	Na_2CO_3	Na_2SiO_3	Na_2CO_3
815 °C	43 ± 3	57 ± 3	52 ± 1	48 ± 1
835 °C	38 ± 4	62 ± 3	45 ± 1	55 ± 1
855 °C	52 ± 3	48 ± 3	53 ± 1	47 ± 1
880 °C	64 ± 3	36 ± 4	64 ± 1	36 ± 1

[a] See text for an explanation of the discrepancy at the lower temperatures.

To understand the mechanism of the reaction in terms of the kinetics of the granular interface, it is useful to focus on the early stages of the reaction. The first deviation from the sodium carbonate reference pattern is almost exclusively due to Na^+ ions in the interface between quartz and sodium carbonate, as no homogeneous product has formed at this stage. The first slices (spectra 3 min into heating) of the metasilicate batch and pure sodium carbonate are compared in Figure 8 at three different temperatures. The spectra near 800 °C (cf. Figure 8a) are below the solidus of all components. Any reaction taking place has to be a solid-state reaction at the grain interface. The batch spectrum is quite similar to the reference because the reaction is rather slow at this temperature. At 815 °C (cf. Figure 8b), both the raw materials and any product would be solid if in thermodynamic equilibrium, but the eutectic on the silica-rich side of the disilicate composition would be molten under equilibrium conditions. However, there is no liquid component in the batch spectrum at 815 °C. The carbonate reference line is noticeably motionally narrowed under these conditions. This does not apply to the batch spectrum, although the majority of the ^{23}Na nuclei still reside in the carbonate phase. Therefore, the broadness of the batch spectrum at 815 °C is more likely to be due to a distribution of environments in the interface than due to a lack of motional narrowing. At 855 °C (cf. Figure 8c), a wide compositional range between disilicate and silica would be molten under equilibrium conditions. The sodium carbonate reference is clearly entirely liquid at this temperature, but the batch spectrum remains broad and has certainly no liquid component. Therefore, the reaction front, driven by fast Na^+ diffusion in the disordered interface, is progressing sufficiently fast through the grain interface to prevent any part of the sample from reaching thermodynamic equilibrium locally. The broadness of the line reflects not only the lack of liquid phases but also the broad range of environments in the interface. This is underlined by the fact that the line width of the reactant component in the in situ spectra increases with heating time (cf. Figure 9). The ^{23}Na nuclei contributing to this component are in a progressively increasing range of chemical environments.

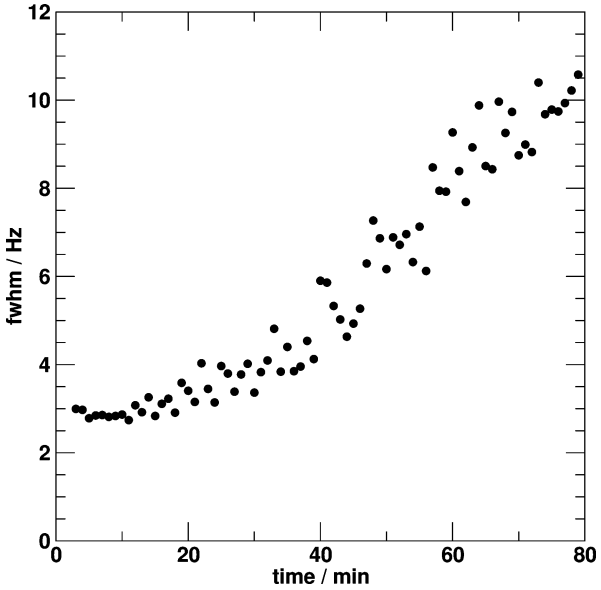

Figure 9. Evolution of the line width of the reactant component in the metasilicate batch at 855 °C.

For the first 20 min, the disilicate batches follow the same reaction pathway as the metasilicate ones. This indicates that the interface between quartz and sodium carbonate grains is the rate-limiting feature rather than the chemical restructuring of the quartz grain cores themselves; the additional quartz does not deplete the Na^+ supply. To establish at what point and how the mechanism in the disilicate batch diverges from the

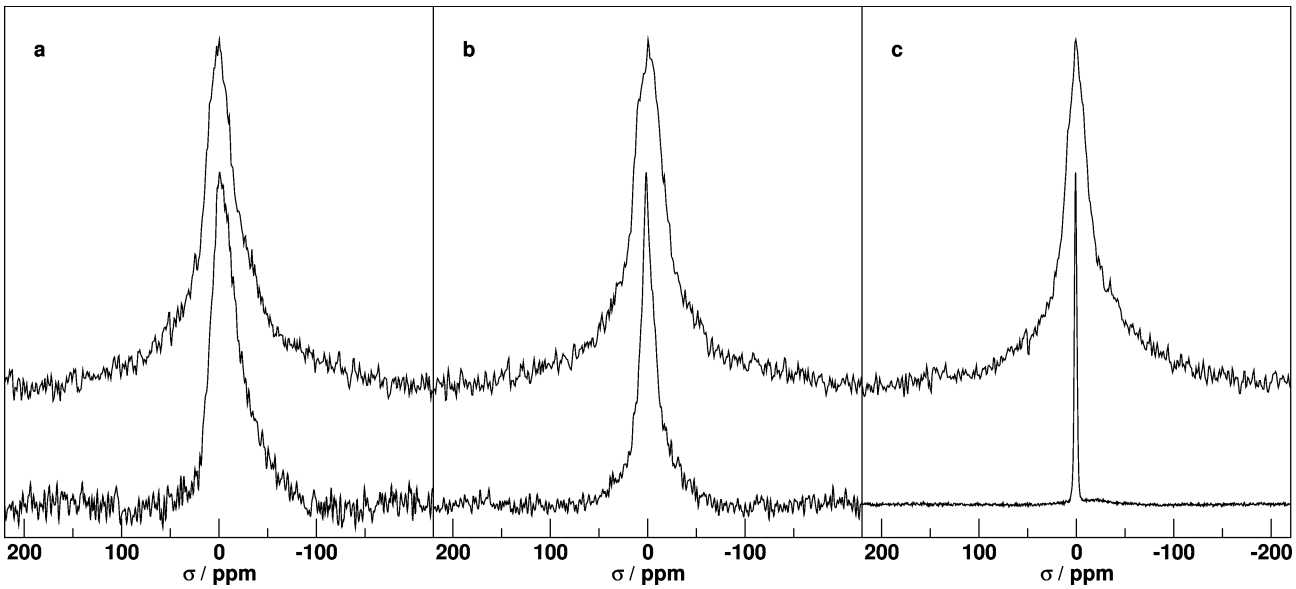

Figure 8. Comparison of the initial stages (slices after 3 min) of the metasilicate batches (top traces) with pure Na_2CO_3 (bottom traces) under similar conditions: (a) 790 °C/815 °C (Na_2CO_3 and batch, respectively); (b) 835 °C; (c) 880 °C. All spectra are scaled to have the same amplitude, hence the different signal-to-noise ratio.

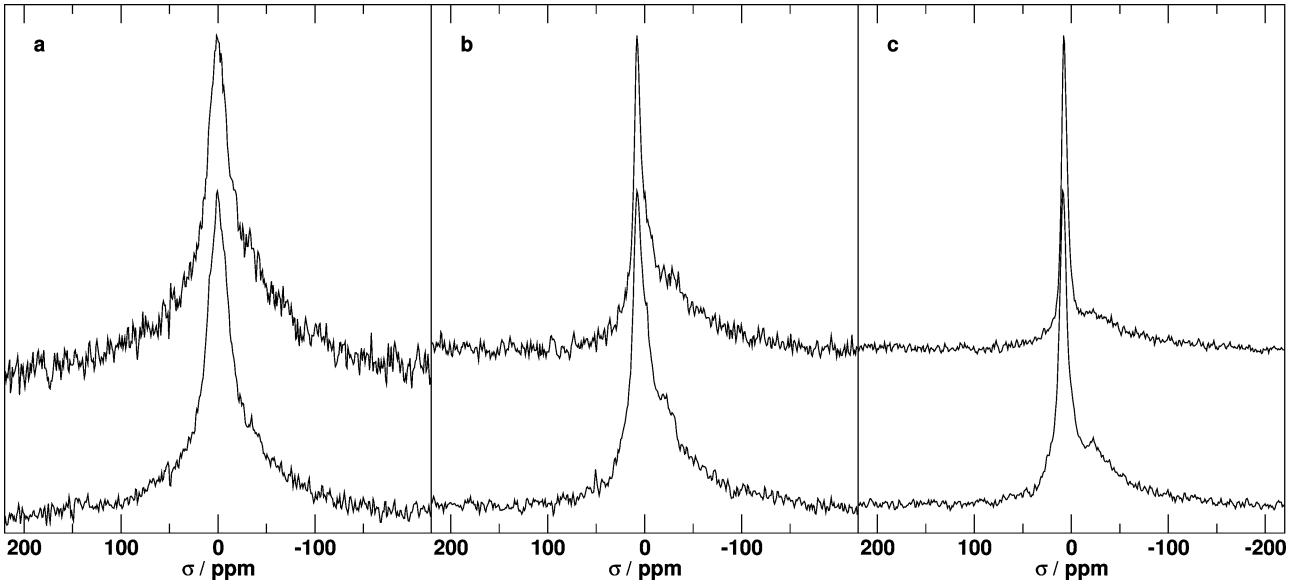

Figure 10. Comparison of the disilicate (top) and metasilicate (bottom) batch line shapes after (a) 3 min, (b) 20 min, and (c) 80 min. The batch reactions take different pathways after ~20 min. All spectra are scaled to have the same amplitude, hence the different signal-to-noise ratio.

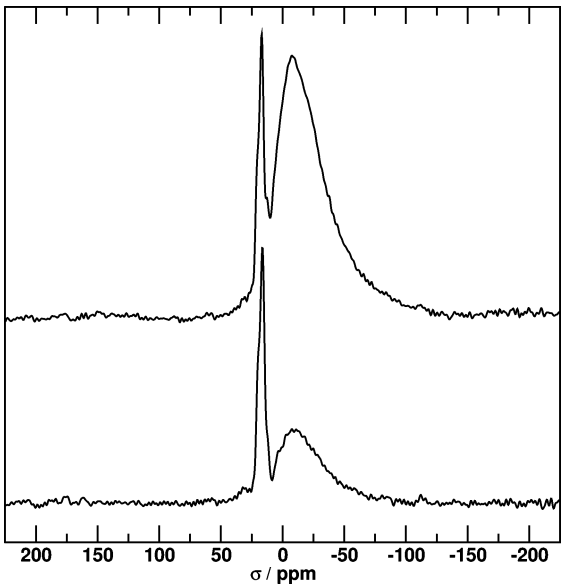

Figure 11. Ex situ ^{23}Na MAS spectra of the quenched disilicate batch after a reaction time of (a) 39 min and (b) 120 min.

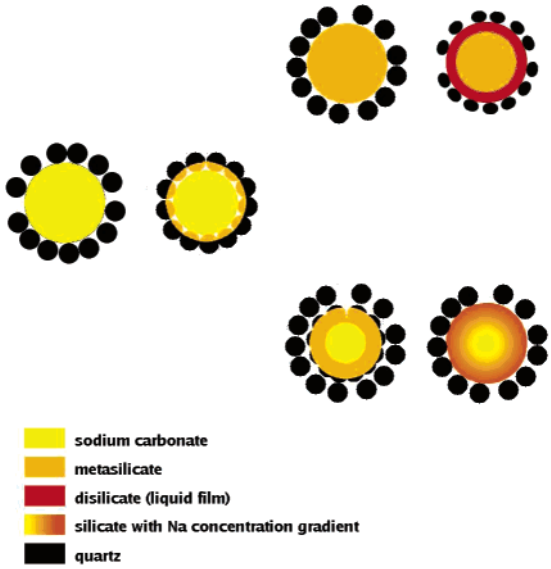

Figure 12. Model of the batch reactions as derived from the in situ NMR experiments. The reaction progresses from left to right. The second step of the disilicate batch reaction, which involves additional SiO_2 grains which were not in contact with the carbonate grain at the outset, follows the upper pathway at high temperatures (i.e., where diffusion is unrestricted) and the lower one at lower temperatures, where diffusion limits the reaction rate. See text for details.

metasilicate case, the slices after 3, 20, and 80 min at 880 °C are compared in Figure 10. A much narrower component begins to grow to the right of the metasilicate line. This line is attributed to liquid disilicate. The MAS spectrum taken after the in situ experiment (cf. Figure 11) confirms that the disilicate batch did in fact melt partially, as it contains a broad Gaussian line consistent with the statistical distribution of sites expected in a disordered structure when there is no motional narrowing present. The fraction of Na^+ ions located in this melt/glass phase is 75% after 39 min and 94% after 120 min. The other, narrow, peak is due to crystalline metasilicate. No unreacted Na_2CO_3 is present after 39 min.

The disilicate batch reaction, visualized in Figure 12, takes place in two steps with quite distinct time scales: In the first step, which is rather fast, nearly all the Na_2CO_3 is consumed to form metasilicate in a solid-state reaction. The second step, in which the intermediate product reacts with the remaining quartz, seems to be inhibited. It only takes place if the temperature is high enough for the disilicate product to be liquid. If this is the case, the formation of a liquid film at the grain interface speeds up diffusion and the reaction is driven to completion. The fact that the formation of liquid disilicate drives the entire batch reaction can be seen from the fact that the first stage, which is identical to the reaction taking place in metasilicate batches, takes place at a higher rate than in metasilicate batches themselves. At 880 °C, the metasilicate batch needs ~41 min to form 67% of metasilicate. After the same time at the same temperature, the disilicate batch has already reacted all Na_2CO_3 and formed a substantial amount of disilicate melt (cf. Figure 11). If, on the other hand, the temperature is too low for a liquid film to form, the Na^+ diffusion in the solid state is too slow. As a consequence, only a distribution of sodium environments, consistent with a concentration gradient across a reaction layer at the grain interface, is observed. This means that the reaction is kinetically controlled at low temperatures, with solid-

state diffusion being the limiting factor. It is thermodynamically controlled at high temperatures, where substantial parts of the sample are above the equilibrium liquidus. This mechanism is also supported by a separate MAS study of disilicate batches heated ex situ and subsequently quenched after various heating times.[17]

An order-of-magnitude calculation of the number of direct grain-to-grain contacts is possible assuming that all grains are spherical with a fixed size of 63 μm (quartz) and 300 μm (Na_2CO_3).[33] The different size of the two raw materials will result in the smaller quartz grains filling the spaces between the larger Na_2CO_3 grains in the batch; hence, the amount of contacts between carbonate grains will be reduced compared to a more even mixture. In this simple geometrical approximation, up to a maximum of 71 quartz grains can have direct contact with a central carbonate grain, corresponding to one monolayer of quartz grains. From the batch compositions, it can be calculated that the metasilicate batch contains 61 "standard" quartz grains per Na_2CO_3 grain, while there are 118 quartz grains available in a disilicate batch. Therefore, the metasilicate batch is close to monolayer coverage and hence the maximum interface area. In the disilicate batch, there is a considerable fraction of quartz grains which are not in direct contact with a sodium source. These can only begin to react as soon as a liquid film has formed, which can wet these excess grains and begin the second stage of the disilicate reaction.

5. Conclusions

In situ high-temperature NMR spectroscopy has been used to investigate the kinetics of the silicate batch reaction. The two main advantages of the technique over ex situ NMR experiments is the high time resolution,[18] which cannot be achieved by preparing separate samples quenched after different times, and the fact that quenching artifacts such as recrystallization or other phase transitions can be ruled out. The main disadvantage is the broadness of the line due to the infeasibility of MAS at sufficiently high temperatures, but this can be overcome by individual MAS experiments on final products and a few quenched samples whose results are used to constrain the fit of the static in situ line shape.

It is clear that, in the future, better temperature measurement is necessary. Pyrometry can certainly help when dealing with samples undergoing phase transitions. If, as in this case, a chemical reaction is studied, the emissivity of the sample will change over time in an unknown and unpredictable fashion. Techniques such as laser-absorption radiation thermometry,[34] which allow one to measure the temperature of a gray body without knowing its emissivity, may be suitable in the future, although more development effort is necessary.

The kinetics of the reactive melting of glass-forming silicate batches was studied using a model system with a fairly narrow grain size distribution. The preferred reaction product is metasilicate. It is formed by solid-state reaction even when the temperature is well above the liquidus of much of the composition space between SiO_2 and $Na_2O{\cdot}2SiO_2$. This means that Na^+ diffusion is fast, allowing the reaction front to proceed very rapidly. Thermodynamic equilibration is lagging behind in this process, so that the liquid equilibrium phase near the eutectic is never reached. This mechanism relies on an ample supply of Na^+ ions and a large interface cross-sectional area. The grain size combination chosen, large Na_2CO_3 grains surrounded by small quartz grains, favors this mechanism.

The observed kinetics of the metasilicate batch reaction is more deceleratory than any of the standard models for diffusion-controlled solid-state reactions. This may be due partly to a thermal gradient in the sample, which would mean that the top layer of the sample is at too low a temperature to react on the time scale of the experiment. However, the observed behavior can be explained under certain conditions if the concentration dependence of the diffusion coefficient and activation energy is being taken into account when solving the diffusion equation.[29]

In disilicate batches, where some of the quartz cannot be in direct contact with a Na^+ source for geometrical reasons, the first stage of reaction is the same as that in the metasilicate batches. After ~20 min, the mechanism changes and a liquid film of disilicate is formed. This melt phase can wet the excess quartz grains and transform the whole sample into liquid disilicate (and subsequently into glass after quenching). It is interesting to note that this second step, where thermodynamics rather than kinetics governs the reaction, drives the entire reaction to such an extent that metasilicate is formed faster as an intermediate in disilicate batches than in metasilicate batches themselves.

Acknowledgment. R.W. and A.R.J. would like to thank Ian Smith, Pilkington European Technical Centre, Ormskirk, and Neville Greaves, UWA, for discussion and support. Access to the high-temperature NMR facility at CRMHT was granted under contract ARI HPRI-CT-1999-00042 from the European Union. A.R.J. would like to thank the UK Engineering and Physical Sciences Research Council and Pilkington for a Ph.D. studentship from the Collaborative Awards in Science and Engineering scheme.

References and Notes

(1) Kim, Y.; Kirkparick, R. J. *Am. Mineral.* **1998**, *83*, 339.
(2) Meneau, F.; Greaves, G. N.; Winter R.; Vaills Y. *J. Non-Cryst. Solids* **2001**, *293*, 693.
(3) Jones, A. R.; Winter R.; Greaves, G. N.; Smith I. H. *J. Non-Cryst. Solids* **2001**, *293*, 87.
(4) Jones, A. R.; Winter, R.; Greaves, G. N.; Targett-Adams, C.; Smith, I. H. *Glass Technol.* **2002**, *43C*, 52.
(5) Robert, E.; Whittington, A.; Fayon, F.; Pichavant, M.; Massiot, D. *Chem. Geol.* **2001**, *174*, 291.
(6) Ratai, E.; Chan J. C. C.; Eckert, H. *Phys. Chem. Chem. Phys.* **2002**, *4*, 3198.
(7) Holland, D.; Howes A. P.; Dupree, R.; Johnson J. A.; Johnson, C. E. *J. Phys.: Condens. Mater.* **2003**, *15*, S2457.
(8) Sen, S.; Youngman R. E. *J. Phys. Chem. B* **2004**, *108*, 7557.
(9) LeMessurier, D. A.; Sissouno, N.; Vearey-Roberts, A.; Evans, S.; Evans, D. A.; Winter, R. *Mater. Sci. Technol.* **2004**, *20*, 975.
(10) Saito, K.; Kanehashi, K.; Saito, Y.; Godward, J. *Appl. Magn. Reson.* **2002**, *22*, 257.
(11) Dajda, N.; Dixon, J. M.; Smith, M. E.; Carthey, N.; Bishop, P. T. *Phys. Rev. B* **2003**, *67*, 024201.
(12) Florian, P.; Massiot, D.; Poe, B.; Farnan, I.; Coutures, J. P. *Solid State Nucl. Magn. Reson.* **1995**, *5*, 233.
(13) Sen, S. *J. Non-Cryst. Solids* **1999**, *253*, 84.
(14) Nuta, L.; Bessada, C.; Veron, E.; Matzen, G. *C. R. Chim.* **2004**, *7*, 395.
(15) George, A. M.; Richet, P.; Stebbins, J. F. *Am. Mineral.* **1998**, *83*, 1277.
(16) Kracek, F. C. *J. Phys. Chem.* **1930**, *34*, 1583.
(17) Jones, A. R.; Winter, R.; Greaves, G. N.; Smith, I. H. Manuscript in preparation.
(18) Winter, R.; Shaw-West, R.; Wolff, M.; Clasen, R.; Broussely, M.; Levick, A. Manuscript in preparation.
(19) Lacassagne, V.; Bessada, C.; Ollivier, B.; Massiot, D.; Florian, P.; Coutures, J.-P. *C. R. Acad. Sci. Paris, Ser. IIb* **1997**, *325*, 91.
(20) Lacassagne, V.; Bessada, C.; Florian, P.; Bouvet, S.; Ollivier, B.; Coutures, J.-P.; Massiot, D. *J. Phys. Chem. B* **2002**, *106*, 1862.
(21) Bessada, C.; Anghel, E. M. *Inorg. Chem.* **2003**, *42*, 3884.

(22) von Barner, J. H.; Bessada, C.; Berg, R. W. *Inorg. Chem.* **2003**, *42*, 1901.
(23) Harris, M. J.; Cowley, R. A.; Swainson, I. P.; Dove, M. T. *Phys. Rev. Lett.* **1993**, *71*, 2939.
(24) Massiot, D.; Fayon, F.; Capron, M.; King, I.; LeCalvé, S.; Alonso, B.; Durand, J.-O.; Bujoli, B.; Gan, Z.; Hoatson, G. *Magn. Reson. Chem.* **2002**, *40*, 70.
(25) Bamford, C. H.; Tipper, C. F. H. *Comprehensive chemical kinetics: Reactions in the solid state*; Elsevier: Amsterdam, The Netherlands, 1980; Vol. 22, p 68 ff.
(26) Ginstling, A. M.; Brounshtein, B. I. *J. Appl. Chem. U.S.S.R. (Engl.)* **1950**, *23*, 1327.
(27) Dickinson, C. F.; Heal, G. R. *Thermochim. Acta* **1999**, *340*, 89.
(28) Verheijen, O. S. *Thermal and chemical behavior of glass forming batches*; Technische Universiteit: Eindhoven, The Netherlands, 2003; p 77 ff.
(29) Winter, R.; Jones, A. R. Manuscript in preparation.
(30) Koller, H.; Engelhardt, G.; Kentgens, A. P. M.; Sauer, J. *J. Phys. Chem.* **1994**, *98*, 1544.
(31) Clark, T. M.; Grandinetti, P. J.; Florian, P.; Stebbins, J. F. *J. Phys. Chem. B* **2001**, *105*, 12257.
(32) Egan, J. M.; Mueller *J. Phys. Chem. B* **2000**, *104*, 9580.
(33) Jones, A. R. *NMR and XRD investigation of glass-forming reactions between quartz and sodium carbonate*; University of Wales: Aberystwyth, U.K., 2003; p 158.
(34) Levick, A.; Edwards, G. *Anal. Sci.* **2001**, *17*, S438.